

High-Pressure Density Measurements for the Binary System Cyclohexane + *n*-Hexadecane in the Temperature Range of (318.15 to 413.15) K

Josinira A. Amorim,[†] Osvaldo Chiavone-Filho,[†] Márcio L. L. Paredes,[‡] and Krishnaswamy Rajagopal^{*,§}

Universidade Federal do Rio Grande do Norte, Departamento de Engenharia Química, PPGEQ, UFRN—Campus Universitário, 3000 CEP 59072-970, Brazil, Universidade do Estado do Rio de Janeiro, PPG-EQ, Instituto de Química, UERJ—Campus Maracanã, PHLC, 411 CEP 20550-900, Brazil, and Universidade Federal do Rio de Janeiro, DEQ, Escola de Química, UFRJ—Ilha do Fundão, CT, I-122 CEP 21949-900, Brazil

The densities of binary mixtures of *n*-hexadecane and cyclohexane at high pressures were measured in the range of (6.895 to 62.053) MPa at six different temperatures varying from (318.15 to 413.15) K and for eight compositions. The measurements were made by a high-pressure Anton Paar DMA 512 P densimeter integrated with the Ruska 2370 mercury Free PVT System. The densimeter was calibrated using analytical grade toluene, cyclohexane, and *n*-heptane as calibration fluids. The experimental error of density measurements is estimated as 0.5 kg·m⁻³. The measured densities at 348.15 K agree well with the available literature values at different pressures. The excess volumes, thermal expansion, and isothermal compressibility coefficients were obtained from measured densities. All data were correlated successfully with a modified Peng–Robinson equation of state.

Introduction

The knowledge of thermophysical properties of mixtures at different pressures and temperatures is relevant in design, operation, control, and optimization of industrial processes. The experimental properties of mixtures can provide valuable information about the fluid behavior at different compositions and help in developing models and correlations. These correlations are necessary as it is impractical to measure properties at all needed compositions, especially in the case of multi-component mixtures.

Among the thermophysical properties, density is especially important due to several formal relations between volumetric properties and other thermodynamic properties. For instance, an accurate modeling of density data at different conditions allows the correct and simple computational extrapolation and interpolation of density as well as other thermodynamic properties such as specific heats. Density has been used traditionally in the characterization of complex mixtures,¹ such as petroleum containing mainly nonpolar substances like long chain alkanes, naphthenic, and aromatic compounds with a wide range of carbon numbers.²

In asymmetric mixtures, large differences in molecular shape, size, or flexibility could cause deviations in physical properties from ideal mixture properties, even for mixtures of nonpolar substances.³ In this work, cyclohexane and *n*-hexadecane were selected for density measurements at high pressures. Cyclohexane is a small naphthenic molecule while *n*-hexadecane is a long linear alkyl chain, leading to an asymmetrical mixture in length and shape of components with close densities at ambient conditions. Cyclohexane is also an important intermediate in the petrochemical industry, and *n*-hexadecane is a common standard for diesel fuel applications.

* Corresponding author. E-mail: raja@eq.ufrj.br. Fax: +55 21 25627567. Phone: +55 21 25627654.

[†] Universidade Federal do Rio Grande do Norte.

[‡] Universidade do Estado do Rio de Janeiro.

[§] Universidade Federal do Rio de Janeiro.

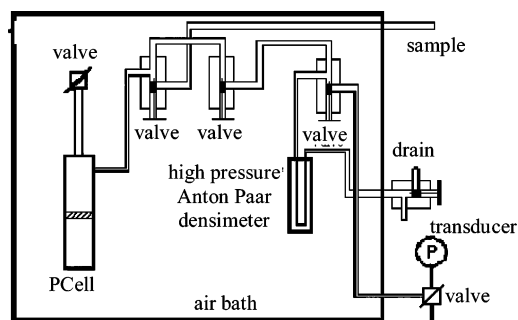


Figure 1. Schematic of the PVT system used to measure high-pressure densities.

With similar premises, Tanaka et al.⁴ measured densities for cyclohexane and *n*-hexadecane mixtures at (298.15, 323.15, and 348.15) K. In this work, high-pressure density data of cyclohexane + *n*-hexadecane mixtures were measured up to 62.053 MPa for a wide range of temperature of (318.15 to 413.15) K using a vibrating-tube densimeter. From the density data, the isobaric thermal expansion and the isothermal compressibility have been determined and reported. The behavior of these properties as a function of temperature, pressure, and composition was studied. Densities were correlated by a novel volume-scaled approach applied to the Peng–Robinson equation of state (EOS).

Experimental Section

Apparatus. The apparatus for high-pressure density measurements is shown schematically in Figure 1. The main cell for our purpose was the pump cell (PCell).

The volume in the PCell can be changed by computer-controlled stepping motors, and it is a function of the piston position. The sample was introduced in the PCell and stirred well. The piston was activated to transfer sample from PCell up to the densimeter and to remove the air from the whole system. The pressure was increased up to 6.895 MPa and

maintained constant at that pressure. The air bath and the temperature control system were activated. After the desired temperature was reached, the monitoring of the oscillation period of the densimeter was done until stabilization was achieved. Density was obtained from measurements of the oscillation period of the sample in a U-shape tube. Using the experimental technique of the vibratory pipe, the density is related with the period of oscillation by

$$\rho(P, T) = A(P, T)\pi^2 + B(P, T)\pi + C(P, T) \quad (1)$$

where P is the pressure; T is the temperature; $\rho(P, T)$ is the mass density of the sample; π is the period of oscillation; and $A(P, T)$, $B(P, T)$, and $C(P, T)$ are constants that are determined using three fluids of calibration of known density in the complete range of pressure and temperature. Three reference fluids were used in order to improve the accuracy of the calibration providing a better correlation (eq 1). The standard fluids of calibration were toluene (TEDIA, 99 % purity), *n*-heptane (Tedia, 99 % purity), and cyclohexane (Tedia, 99 % purity). Equation 1 correlated the densities of the standard fluids within a root mean square deviation (rmsd) of $0.3 \text{ kg}\cdot\text{m}^{-3}$ as compared to the reference densities of these substances from NIST (National Institute of Standards and Technology).⁵ The maximum absolute deviation of the reference NIST densities when compared to the experimental data of cyclohexane in the literature,⁶ in the range of (313.15 to 323.15) K and (5 to 15) MPa, is $0.14 \text{ kg}\cdot\text{m}^{-3}$.

Measurement of Density. Commercially available analytical grade cyclohexane (TEDIA, 99 % purity) and *n*-hexadecane (VETEC, 99 % purity) were used without any further purification. The binary mixtures were prepared immediately before use by weighing in a Sartorius precision digital balance at atmospheric pressure and ambient temperature with an uncertainty of $1 \times 10^{-7} \text{ kg}$. The measurement of density was made using a high-pressure Anton Paar DMA 512 P vibrating-tube densimeter integrated with the Ruska 2370 mercury Free PVT System as a function of pressure (P), temperature (T), and mole fraction (x). At least 10 values were taken for each pressure at a given temperature.

The reproducibility of density was within $0.5 \text{ kg}\cdot\text{m}^{-3}$. The uncertainties of P , T , and x were $7 \times 10^{-4} \text{ MPa}$, 0.1 K , and 3×10^{-6} , respectively. No viscosity correction was necessary⁷ for density measurements by a DMA 512 P vibrating-tube densimeter as the viscosities of the standard and measured fluids were less than $15 \text{ mPa}\cdot\text{s}$. The densities studied in this work were obtained in the temperature range of (318.15 to 413.15) K and the pressure range of (6.895 to 62.053) MPa for eight different compositions.

Volumetric Properties. The isobaric thermal expansion (α), the isothermal compressibility coefficients (k_T), and excess volume (V^E) were derived from experimental densities. These properties are defined, respectively, in eqs 2 to 4:

$$\alpha(P, T, x) = -\frac{1}{\rho} \left(\frac{\partial \rho}{\partial T} \right)_{P,x} \quad (2)$$

$$k_T(P, T, x) = \frac{1}{\rho} \left(\frac{\partial \rho}{\partial P} \right)_{T,x} \quad (3)$$

$$V^E(P, T, x) = V(P, T, x) - (x_1 V_1(P, T) + (1 - x_1) V_2(P, T)) \quad (4)$$

where subscripts 1 and 2 stand for the pure components cyclohexane and *n*-hexadecane, respectively; V is the molar volume of the mixture.

The values of α were estimated from cubic polynomial correlation of density as a function of temperature at constant pressure and composition. Similarly, k_T was estimated from cubic polynomial correlation of density as a function of pressure at constant temperature and composition. The overall rmsd between calculated and experimental density was $0.30 \text{ kg}\cdot\text{m}^{-3}$ and $0.08 \text{ kg}\cdot\text{m}^{-3}$ for the density correlations as functions of temperature and pressure, respectively.

Modeling. The Peng–Robinson⁸ EOS was adapted in order to correlate the experimental data following an approach recently developed by Amorim et al.⁹ The equations used are presented in eqs 5 and 6:

$$P = \frac{RT}{V-b} - \frac{a(T)}{V^2 + 2bV - b^2}; \quad a(T) = c[1 + k(1 - \sqrt{T/\tau})]^2 \quad (5)$$

$$c = 0.4572355 \frac{(R\tau)^2}{\Pi}; \quad b = 0.07779607 \frac{R\tau}{\Pi};$$

$$k = 0.37464 + 1.54226\Omega - 0.26992\Omega^2 \quad (6)$$

where R is the universal gas constant; c , b , and k are auxiliary functions; and τ , Π , and Ω are pure components model parameters. τ and Π have the dimension of temperature and pressure, while Ω has no dimension.

In a preliminary study, the Peng–Robinson EOS was used in order to correlate density data at several pressures and at fixed T and x . This EOS was not able to accurately represent density and k_T simultaneously, even using τ , Π , and Ω as estimated parameters instead of the physical properties critical temperature, critical pressure, and acentric factor, respectively. In order to improve the modeling, an approach similar to volume translation was used: the density calculated from the original EOS was used as input in the final calculation of density. The strategy adopted was to obtain τ , Π , and Ω so that k_T was as well correlated as possible. After that, the relation between calculated and experimental density was investigated, and a simple volume scaling was applied, as presented in eq 7, where M is the molecular weight:

$$\rho^{\text{calc}} = \frac{a^s(T)}{M} \rho^{\text{EOS}}; \quad a^s(T) = a_0^s + \frac{a_1^s}{T} \quad (7)$$

where $a^s(T)$ is a scaling function; a_0^s and a_1^s are pure component model parameters.

The volume-scaled Peng–Robinson EOS is hereafter referred to as VS-PR. The mixing rules used were

$$a(T) = \sum_i \sum_j x_i x_j a_{ij}(T); \quad b = \sum_i \sum_j x_i x_j b_{ij};$$

$$a^s(T) = \sum_i \sum_j x_i x_j a_{ij}^s(T) \quad (8)$$

and the combining rules were

$$a_{ij}(T) = \sqrt{a_i(T)a_j(T)} (1 - k_{ij}); \quad b_{ij} = \frac{b_i + b_j}{2} (1 - l_{ij});$$

$$a_{ij}^s(T) = \frac{a_i^s(T) + a_j^s(T)}{2} (1 - m_{ij}) \quad (9)$$

The parameters in eq 6 (τ , Π , and Ω for each pure component), eq 7 (a_0^s and a_1^s for each pure component), and eq 9 (k_{12} , l_{12} ,

Table 1. Experimental Density Data (in $\text{kg}\cdot\text{m}^{-3}$) for the System Cyclohexane (1) + *n*-Hexadecane (2) at Different Pressures, Temperatures, and Compositions

<i>P</i>	<i>x</i> ₁								
	1	0.9000	0.8000	0.7000	0.5000	0.3000	0.2000	0.1002	0
<i>T</i> /K = 318.15									
6.895	761.5	758.5	758.1	757.6	758.6	759.6	760.3	760.3	
13.789	767.7	764.6	763.6	763.3	763.9	763.9	765.1	765.0	
20.684	773.8	770.3	768.9	768.2	768.8	768.9	769.8	769.6	
27.579	779.0	775.3	773.8	772.9	773.2	773.5	773.9	773.9	
34.474	784.1	780.0	778.4	777.6	777.6	777.7	778	777.7	
41.369	788.7	784.6	782.9	781.8	781.6	781.5	781.8	781.5	
48.263	793.4	788.8	786.9	785.8	785.5	785.4	785.5	785.2	
55.158	797.4	792.9	790.7	789.4	789.0	788.8	788.8	788.7	
62.053	801.4	796.7	794.6	793.2	792.5	792.3	792.2	791.7	
<i>T</i> /K = 333.15									
6.895	747.3	745.9	746.6	746.2	747.8	749.3	750.4	750.7	
13.789	754.1	752.3	752.8	752.1	753.5	754.4	755.8	755.8	
20.684	760.5	758.4	758.4	757.6	758.6	759.5	760.4	760.4	
27.579	766.5	763.8	763.6	762.7	763.6	764.1	765.0	765.1	
34.474	772.0	768.9	768.6	767.5	768.3	768.3	769.5	769.7	
41.369	777.0	773.9	773.3	772.1	772.5	772.4	773.4	773.9	
48.263	781.7	778.7	777.5	776.1	776.6	776.5	777.2	777.6	
55.158	786.3	783.2	781.9	780.6	780.5	780.4	781.0	781.2	
62.053	790.7	787.3	786.0	784.2	784.1	783.8	784.4	784.3	
<i>T</i> /K = 348.15									
6.895	733.6	734.7	735.7	735.7	737.5	739.8	740.4	741.3	741.7
13.789	741.2	741.9	742.4	742.3	743.5	745.6	745.9	747.0	747.2
20.684	748.2	748.3	748.3	748.1	749.1	751.0	751.1	752.1	752.5
27.579	754.5	754.3	754.3	753.7	754.3	756.1	756.3	757.2	757.2
34.474	760.5	760.0	759.6	758.9	758.9	760.7	760.8	761.8	761.9
41.369	766.1	765.2	764.6	763.6	763.9	765.3	765.1	766.1	766.1
48.263	771.4	770.0	769.3	768.3	768.2	769.5	769.2	770.2	770.2
55.158	776.2	774.6	773.8	772.6	772.3	773.4	773.5	773.9	774.1
62.053	781.1	779.1	777.9	776.8	776.3	777.2	777.2	777.5	777.6
<i>T</i> /K = 363.15									
6.895	719.6	722.6	724.5	725.0	727.0	729.8	731.4	732.0	
13.789	727.9	730.3	731.8	732.2	733.6	736.2	737.5	738.1	
20.684	735.7	737.5	738.4	738.6	739.4	742.0	743.3	743.9	
27.579	742.8	744.2	744.5	744.3	745.1	747.2	748.4	748.6	
34.474	749.1	750.3	750.3	749.8	750.3	752.4	753.4	753.7	
41.369	755.3	755.7	755.7	755.2	755.5	757	758.1	758.4	
48.263	760.7	760.9	760.6	760.0	760.1	761.6	762.5	762.6	
55.158	765.8	765.8	765.3	764.6	764.4	765.7	766.6	766.7	
62.053	771.0	770.6	770.1	768.8	768.6	769.7	770.4	770.5	
<i>T</i> /K = 388.15									
6.895	694.7	700.0	702.0	704.3	709.5	711.7	714.0	714.7	
13.789	705.0	709.3	710.2	712.6	717.1	718.9	721.2	721.7	
20.684	713.9	717.5	718.2	720.0	723.8	725.5	727.6	728.1	
27.579	721.9	724.8	725	726.8	730.3	731.6	733.4	733.9	
34.474	729.2	731.8	731.6	732.7	736.1	737.1	739.0	739.2	
41.369	736.0	738.1	737.4	738.4	741.2	742.2	744.1	744.1	
48.263	742.2	743.7	743.0	743.5	746.5	747.2	748.7	748.8	
55.158	747.8	749.3	748.0	748.5	751.5	751.8	753.1	753.3	
62.053	753.2	754.3	753.0	753.4	755.7	755.9	757.3	757.5	
<i>T</i> /K = 413.15									
6.895	669.7	675.9	680.0	682.0	687.7	692.4	694.6	696.2	
13.789	682.1	687.0	690.3	691.7	696.7	700.9	702.9	704.3	
20.684	692.5	696.8	699.3	700.2	704.6	708.2	710.0	711.0	
27.579	701.8	705.2	707.2	707.7	711.5	714.9	717.0	717.9	
34.474	710.1	713.0	714.6	714.8	718.2	721.2	723.0	723.7	
41.369	717.7	719.7	721.3	721.2	724.1	726.9	728.8	729.4	
48.263	724.9	726.7	727.3	726.8	729.7	732.3	734.0	734.5	
55.158	731.2	732.5	733.1	732.4	734.9	737.1	738.8	739.5	
62.053	737.2	737.8	738.2	737.4	739.7	741.7	743.2	743.8	

and m_{12}) were obtained by minimization of the sum of square deviations between calculated and experimental densities.

Results and Discussion

The densities of cyclohexane, *n*-hexadecane, and their binary mixtures from (318.15 to 413.15) K and in the pressure range from (6.895 to 62.053) MPa are presented in Table 1. The experimental densities at 348.15 K are compared with the data of Tanaka et al.⁴ in Figures 2 and 3.

The deviation between the data of Tanaka et al.⁴ and of this work is shown in Figure 4. The deviation is within $0.7 \text{ kg}\cdot\text{m}^{-3}$ for the mixtures and in the range of (0.6 to 1.6) $\text{kg}\cdot\text{m}^{-3}$ for

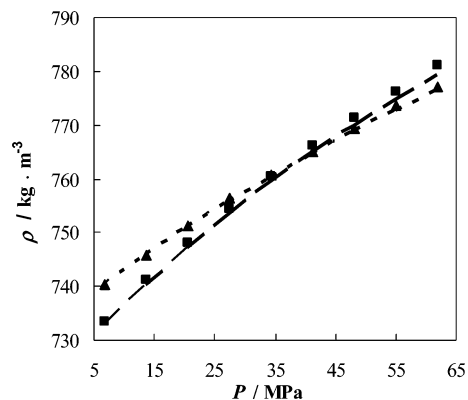


Figure 2. Experimental density of cyclohexane (1) + *n*-hexadecane (2) binary mixtures as a function of pressure in two mole fractions at 348.15 K: ■ and dashed line, $x_1 = 1$; ▲ and dotted lines, $x_1 = 0.2$. Symbols are for data from this work, and lines are from Tanaka et al.⁴

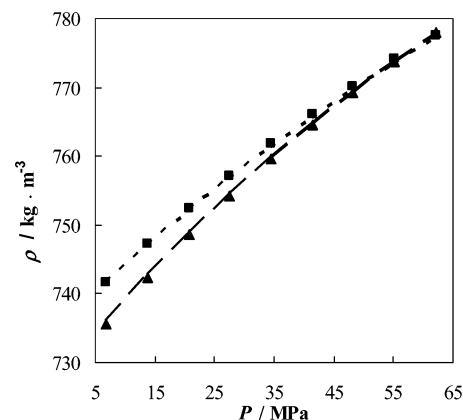


Figure 3. Experimental density of cyclohexane (1) + *n*-hexadecane (2) binary mixtures as a function of pressure in two mole fractions at 348.15 K: ■ and dotted line, $x_1 = 0$; ▲ and dashed line, $x_1 = 0.8$. Symbols are for data obtained in this work, and lines are from Tanaka et al.⁴

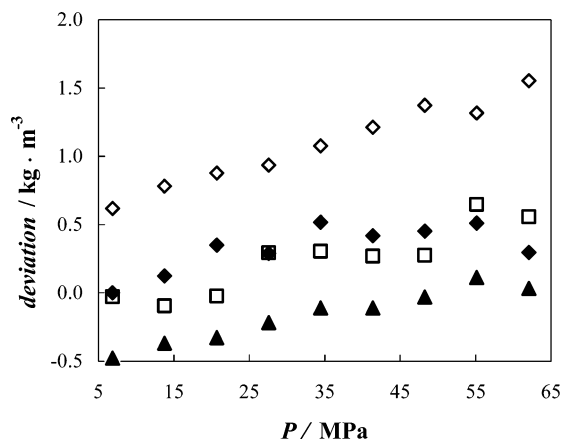


Figure 4. Deviation of experimental densities compared with data obtained from Tanaka et al.⁴ at 348.15 K: ◇, $x_1 = 1$; ◆, $x_1 = 0$; □, $x_1 = 0.2$; ▲, $x_1 = 0.8$.

pure cyclohexane. However, the data of cyclohexane in this work agreed with the reference data⁶ with a rmsd of $0.2 \text{ kg}\cdot\text{m}^{-3}$.

The parameters utilized in the proposed VS-PR are given in Tables 2 and 3. The average rmsd for the estimates from VS-PR were ($0.9, 0.8, 0.3, 0.5, 0.7,$ and 0.7) $\text{kg}\cdot\text{m}^{-3}$, respectively, for temperatures (318.15, 333.15, 348.15, 363.15, 388.15, and 413.15 K) and ($0.7, 0.7, 0.7, 0.7, 0.7, 0.6, 0.7, 0.7,$ and 0.8) $\text{kg}\cdot\text{m}^{-3}$ as average rmsd, respectively, for pressures (6.895, 13.790, 20.684, 27.579, 34.474, 41.369, 48.263, 55.158, and 62.053) MPa. The overall rmsd for VS-PR was $0.7 \text{ kg}\cdot\text{m}^{-3}$.

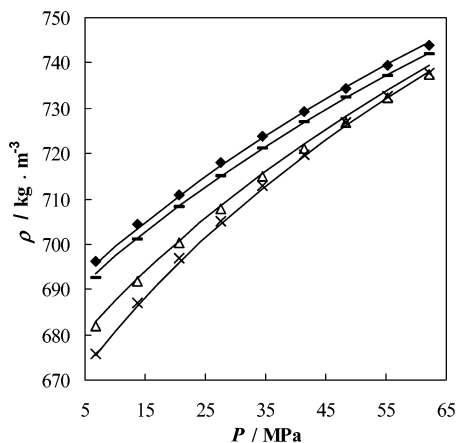


Figure 5. Density of cyclohexane (1) + *n*-hexadecane (2) mixtures as a function of pressure at 413.15 K at various mole fractions: \blacklozenge , $x_1 = 0$; \triangle , $x_1 = 0.3$; \times , $x_1 = 0.7$; \circ , $x_1 = 0.9$; solid lines, calculated with proposed model VS-PR.

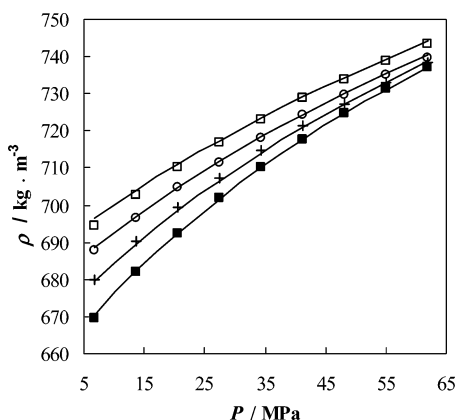


Figure 6. Density of cyclohexane (1) + *n*-hexadecane (2) mixtures as a function of pressure at 413.15 K at various mole fractions: \square , $x_1 = 0.1$; \circ , $x_1 = 0.5$; $+$, $x_1 = 0.8$; \blacksquare , $x_1 = 1$; solid lines, calculated with proposed model VS-PR.

Table 2. Estimated Coefficients Used in Equations 6 and 7

component	Π		τ	Ω	a_0^s	a_1^s
	MPa	K	K		$\text{kg}\cdot\text{mol}^{-1}$	$\text{K}\cdot\text{kg}\cdot\text{mol}^{-1}$
cyclohexane	19.956	628.9	-0.3797	0.021365	-0.183	
<i>n</i> -hexadecane	41.785	758.3	-0.5246	0.013451	-0.342	

Table 3. Estimated Coefficients Used in Equation 9

mixture parameter	k_{12}	l_{12}	m_{12}
		-0.327	-0.186

In order to illustrate the quality of the correlation, in Figures 5 and 6, the experimental densities are compared with the densities estimated by proposed VS-PR at the highest T (413.15 K, where the rmsd is typical) and all compositions. At the highest T and constant P , density was observed to decrease with increasing cyclohexane composition, within the experimental accuracy. On the other hand, at the lowest T (318.15 K) and constant P , density varies not monotonically with composition up to 27.579 MPa and increasing monotonically with increasing cyclohexane composition above 41.369 MPa. At all temperatures, at constant composition, the density increases with increasing pressure, consistent with thermodynamic requirements of stability.

Isothermal compressibility and isobaric expansibility data obtained from experimental density in the studied ranges of pressure and temperature are presented in Tables 4 and 5. The

Table 4. Isothermal Compressibility $k_T \times 10^3/\text{MPa}^{-1}$ Values Calculated from Experimental Density Data

P MPa	x_1							
	1	0.9000	0.8000	0.7000	0.5000	0.3000	0.1002	0
$T/\text{K} = 318.15$								
6.895	1.25	1.21	1.11	1.09	1.04	0.95	0.95	0.94
13.789	1.14	1.10	1.03	1.01	0.96	0.90	0.89	0.88
20.684	1.05	1.01	0.96	0.94	0.89	0.85	0.83	0.83
27.579	0.97	0.93	0.89	0.87	0.83	0.81	0.78	0.77
34.474	0.90	0.86	0.83	0.81	0.77	0.76	0.73	0.73
41.369	0.84	0.80	0.78	0.76	0.73	0.72	0.69	0.68
48.263	0.79	0.76	0.74	0.71	0.68	0.67	0.65	0.64
55.158	0.74	0.73	0.70	0.68	0.65	0.64	0.62	0.60
62.053	0.71	0.70	0.68	0.65	0.63	0.60	0.59	0.57
$T/\text{K} = 333.15$								
6.895	1.40	1.28	1.24	1.19	1.13	1.04	1.03	0.96
13.789	1.28	1.18	1.13	1.10	1.05	0.96	0.96	0.94
20.684	1.17	1.10	1.04	1.02	0.97	0.88	0.88	0.91
27.579	1.07	1.02	0.96	0.94	0.90	0.80	0.81	0.86
34.474	0.99	0.96	0.90	0.88	0.84	0.72	0.73	0.81
41.369	0.92	0.90	0.85	0.82	0.79	0.65	0.66	0.76
48.263	0.86	0.85	0.80	0.78	0.74	0.57	0.59	0.69
55.158	0.81	0.81	0.78	0.74	0.70	0.50	0.52	0.62
62.053	0.77	0.77	0.76	0.70	0.66	0.42	0.45	0.53
$T/\text{K} = 348.15$								
6.895	1.56	1.46	1.36	1.32	1.21	1.16	1.14	1.12
13.789	1.42	1.33	1.25	1.21	1.12	1.08	1.06	1.04
20.684	1.30	1.21	1.15	1.11	1.04	1.01	0.98	0.97
27.579	1.19	1.11	1.06	1.02	0.97	0.94	0.92	0.90
34.474	1.10	1.03	0.98	0.95	0.91	0.88	0.85	0.84
41.369	1.02	0.95	0.92	0.89	0.85	0.82	0.79	0.79
48.263	0.96	0.89	0.86	0.84	0.80	0.77	0.74	0.74
55.158	0.90	0.84	0.81	0.81	0.76	0.73	0.69	0.69
62.053	0.87	0.81	0.77	0.78	0.72	0.69	0.64	0.66
$T/\text{K} = 363.15$								
6.895	1.78	1.65	1.51	1.45	1.32	1.29	1.25	1.24
13.789	1.60	1.49	1.37	1.33	1.23	1.19	1.16	1.14
20.684	1.45	1.35	1.25	1.21	1.14	1.09	1.07	1.05
27.579	1.31	1.22	1.15	1.11	1.06	1.01	0.99	0.98
34.474	1.20	1.12	1.06	1.03	0.99	0.94	0.92	0.91
41.369	1.10	1.03	0.99	0.96	0.92	0.88	0.86	0.85
48.263	1.02	0.96	0.93	0.89	0.87	0.82	0.80	0.79
55.158	0.96	0.91	0.89	0.85	0.81	0.78	0.76	0.75
62.053	0.92	0.87	0.86	0.81	0.77	0.75	0.71	0.71
$T/\text{K} = 388.15$								
6.895	2.21	1.99	1.82	1.82	1.60	1.52	1.50	1.49
13.789	1.96	1.78	1.64	1.60	1.45	1.38	1.36	1.34
20.684	1.74	1.59	1.48	1.42	1.32	1.26	1.24	1.21
27.579	1.55	1.43	1.35	1.27	1.20	1.15	1.13	1.10
34.474	1.39	1.29	1.23	1.14	1.11	1.06	1.03	1.00
41.369	1.26	1.18	1.12	1.05	1.02	0.98	0.95	0.93
48.263	1.15	1.09	1.04	0.99	0.95	0.91	0.88	0.88
55.158	1.07	1.02	0.97	0.95	0.90	0.85	0.83	0.84
62.053	1.01	0.97	0.91	0.94	0.85	0.80	0.78	0.82
$T/\text{K} = 413.15$								
6.895	2.77	2.49	2.27	2.15	1.95	1.81	1.77	1.69
13.789	2.40	2.18	2.01	1.90	1.74	1.62	1.60	1.53
20.684	2.09	1.91	1.78	1.68	1.55	1.46	1.45	1.39
27.579	1.83	1.68	1.58	1.49	1.39	1.32	1.31	1.27
34.474	1.62	1.49	1.41	1.34	1.26	1.20	1.19	1.16
41.369	1.45	1.34	1.27	1.21	1.15	1.09	1.08	1.06
48.263	1.33	1.22	1.16	1.12	1.06	1.00	0.98	0.98
55.158	1.24	1.14	1.08	1.04	0.99	0.94	0.90	0.92
62.053	1.19	1.08	1.02	1.00	0.94	0.88	0.83	0.86

isothermal compressibility increases with x_1 at constant P and decreases with P at constant x_1 . This is shown in Figure 7 at 348.15 K. Analogous results can be obtained at other temperatures. In Figures 7 and 8, the isobaric expansibility and the isothermal compressibility are shown at same conditions, and the same trends with x_1 and P are observed for all T . Again, the VS-PR EOS was utilized in the correlation with very good results, presenting overall rmsd of $1.6 \times 10^{-4} \text{ K}^{-1}$ and $3.6 \times 10^{-5} \text{ MPa}^{-1}$ for isobaric expansibility and the isothermal compressibility, respectively.

In Figures 9 and 10, excess volumes are shown as a function of composition at (318.15 and 363.15) K, respectively, and at five pressures. At the lowest temperature, 318.15 K, the excess volumes decrease initially when adding small amounts of

Table 5. Thermal Expansibility $\alpha \times 10^3/\text{K}^{-1}$ Values Calculated from Experimental Density Data

T K	x_1							
	1	0.9000	0.8000	0.7000	0.5000	0.3000	0.1002	0
<i>P</i> /MPa = 6.895								
318.15	1.20	1.04	0.90	0.96	1.02	0.87	0.85	0.81
333.15	1.24	1.06	0.98	0.96	0.94	0.88	0.85	0.83
348.15	1.28	1.10	1.06	0.99	0.91	0.90	0.87	0.86
363.15	1.33	1.16	1.14	1.05	0.93	0.94	0.91	0.90
388.15	1.43	1.32	1.25	1.20	1.09	1.04	1.02	0.99
413.15	1.55	1.55	1.36	1.44	1.41	1.20	1.21	1.13
<i>P</i> /MPa = 13.789								
318.15	1.15	1.00	0.83	0.92	0.97	0.81	0.81	0.76
333.15	1.17	1.01	0.93	0.92	0.90	0.82	0.80	0.78
348.15	1.20	1.03	1.01	0.93	0.86	0.84	0.82	0.81
363.15	1.23	1.08	1.08	0.98	0.88	0.88	0.85	0.84
388.15	1.30	1.20	1.16	1.11	1.01	0.97	0.95	0.93
413.15	1.37	1.40	1.19	1.33	1.30	1.10	1.12	1.05
<i>P</i> /MPa = 20.684								
318.15	1.11	0.97	0.80	0.88	0.95	0.78	0.79	0.76
333.15	1.12	0.96	0.88	0.87	0.87	0.78	0.77	0.75
348.15	1.13	0.97	0.95	0.88	0.83	0.80	0.77	0.76
363.15	1.15	1.01	1.01	0.92	0.83	0.83	0.80	0.79
388.15	1.20	1.11	1.08	1.04	0.95	0.92	0.90	0.89
413.15	1.27	1.29	1.11	1.25	1.21	1.05	1.08	1.05
<i>P</i> /MPa = 27.579								
318.15	1.04	0.91	0.77	0.85	0.92	0.77	0.74	0.74
333.15	1.06	0.91	0.84	0.83	0.83	0.76	0.73	0.73
348.15	1.07	0.92	0.91	0.84	0.78	0.77	0.74	0.74
363.15	1.09	0.96	0.96	0.87	0.79	0.79	0.77	0.76
388.15	1.13	1.05	1.02	0.99	0.91	0.87	0.85	0.83
413.15	1.17	1.21	1.03	1.20	1.18	1.00	0.98	0.95
<i>P</i> /MPa = 34.474								
318.15	1.00	0.86	0.73	0.82	0.90	0.76	0.72	0.67
333.15	1.01	0.86	0.80	0.81	0.81	0.74	0.70	0.68
348.15	1.03	0.87	0.86	0.81	0.75	0.73	0.71	0.71
363.15	1.04	0.90	0.91	0.84	0.75	0.75	0.73	0.74
388.15	1.06	1.00	0.97	0.94	0.86	0.83	0.82	0.81
413.15	1.08	1.15	0.98	1.10	1.12	0.97	0.95	0.91
<i>P</i> /MPa = 41.369								
318.15	0.95	0.85	0.71	0.78	0.83	0.71	0.69	0.64
333.15	0.96	0.83	0.78	0.77	0.76	0.70	0.68	0.66
348.15	0.97	0.84	0.83	0.78	0.73	0.71	0.68	0.68
363.15	0.99	0.86	0.88	0.81	0.73	0.73	0.70	0.71
388.15	1.01	0.96	0.92	0.90	0.83	0.80	0.78	0.77
413.15	1.04	1.12	0.92	1.05	1.05	0.92	0.90	0.85
<i>P</i> /MPa = 48.263								
318.15	0.93	0.80	0.68	0.75	0.82	0.70	0.67	0.62
333.15	0.94	0.80	0.74	0.74	0.74	0.68	0.66	0.64
348.15	0.94	0.81	0.80	0.75	0.70	0.68	0.66	0.66
363.15	0.95	0.84	0.84	0.78	0.70	0.70	0.68	0.69
388.15	0.96	0.90	0.88	0.87	0.80	0.77	0.75	0.75
413.15	0.96	1.01	0.89	1.02	1.03	0.89	0.87	0.81
<i>P</i> /MPa = 55.158								
318.15	0.87	0.78	0.62	0.70	0.80	0.66	0.65	0.60
333.15	0.90	0.77	0.71	0.71	0.71	0.65	0.63	0.62
348.15	0.91	0.78	0.78	0.73	0.67	0.66	0.64	0.64
363.15	0.92	0.80	0.82	0.76	0.67	0.68	0.66	0.67
388.15	0.92	0.87	0.85	0.84	0.77	0.75	0.72	0.72
413.15	0.90	0.99	0.82	0.96	1.01	0.86	0.84	0.78
<i>P</i> /MPa = 62.053								
318.15	0.82	0.74	0.62	0.69	0.77	0.65	0.64	0.60
333.15	0.86	0.74	0.69	0.69	0.69	0.64	0.62	0.60
348.15	0.88	0.75	0.75	0.70	0.65	0.64	0.62	0.61
363.15	0.90	0.78	0.79	0.73	0.65	0.66	0.63	0.63
388.15	0.89	0.85	0.83	0.82	0.75	0.73	0.71	0.70
413.15	0.86	0.97	0.83	0.95	0.98	0.84	0.84	0.79

cyclohexane to *n*-hexadecane at all pressures. The deviations from ideality are asymmetrical with a maximum found at around 0.7 mole fraction in cyclohexane. However, at intermediate temperatures, (348.15 and 363.15) K, the experimental data exhibit positive and symmetrical behavior. At higher temperatures, (388.15 and 413.15) K, the system again presents asymmetrical behavior similar to that found at lower temperatures.

VS-PR EOS predicts the magnitude of the excess volume. The equation shows a small initial decrease of excess volumes

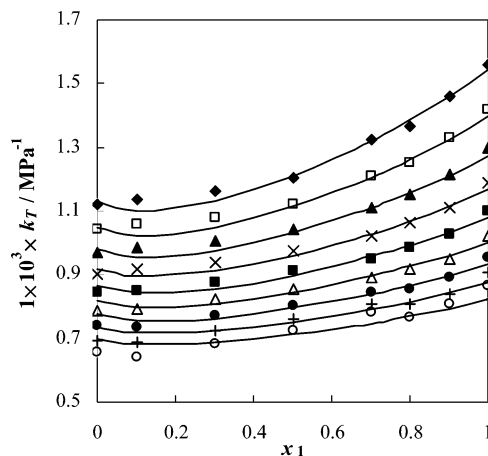


Figure 7. Isothermal compressibility (k_T) vs mole fraction (x_1) for cyclohexane (1) + *n*-hexadecane (2) at 348.15 K: \blacklozenge , 6.895 MPa; \square , 13.789 MPa; \blacktriangle , 20.684 MPa; \times , 27.579 MPa; \blacksquare , 34.474 MPa; \triangle , 41.369 MPa; \bullet , 48.263 MPa; $+$, 55.158 MPa; \circ , 62.053 MPa. Solid lines are calculated values with VS-PR.

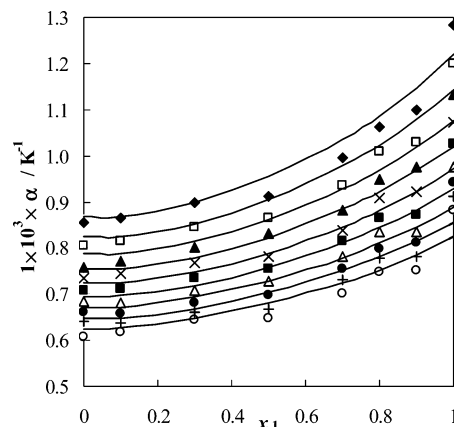


Figure 8. Isobaric expansibility (α) vs mole fraction (x_1) for cyclohexane (1) + *n*-hexadecane (2) at 348.15 K: \blacklozenge , 6.895 MPa; \square , 13.789 MPa; \blacktriangle , 20.684 MPa; \times , 27.579 MPa; \blacksquare , 34.474 MPa; \triangle , 41.369 MPa; \bullet , 48.263 MPa; $+$, 55.158 MPa; \circ , 62.053 MPa. Solid lines are calculated values with VS-PR.

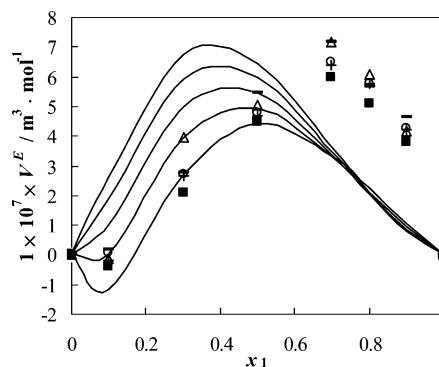


Figure 9. Excess volume versus mole fraction of binary mixture cyclohexane (1) + *n*-hexadecane (2) at 318.15 K: $-$, 6.895 MPa; \triangle , 20.684 MPa; $+$, 34.474 MPa; \circ , 48.263 MPa; \blacksquare , 62.0528 MPa. Solid lines are calculated values with VS-PR.

at pressures up to 13.789 MPa and all temperatures. The predicted maximum deviation is positive and is around 0.3 mole fraction in cyclohexane. The values of experimental excess volumes are quite low and close to the experimental uncertainty, which was about $2 \times 10^{-7} \text{ m}^3 \cdot \text{mol}^{-1}$, leading to a great relative error, making quantitative comparisons difficult.

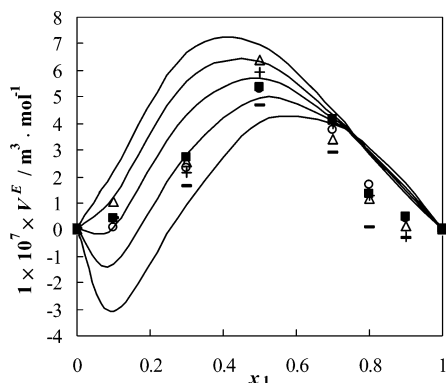


Figure 10. Excess volume versus mole fraction of binary mixture cyclohexane (1) + *n*-hexadecane (2) at 363.15 K. —, 6.895 MPa; Δ , 20.684 MPa, +, 34.474 MPa, \circ , 48.263 MPa \blacksquare , 62.0528 MPa. Solid lines are calculated values with VS-PR.

Conclusion

The densities of cyclohexane, *n*-hexadecane, and their mixtures have been measured in the temperature range of (318.15 to 413.15) K and pressures up to 62.053 MPa. The isothermal compressibility, isobaric expansibility, and excess molar volume were obtained from experimental density data. Density measurements over a wide range of temperature improved the isobaric expansibility data. Density values of this work were compared to values in the literature for this binary system and were found to agree within the experimental uncertainty of $0.7 \text{ kg}\cdot\text{m}^{-3}$.

The VS-PR equation correlated very well the experimental density, isothermal compressibility, and isobaric expansion coefficient when τ , Π , Ω , a_0^s , and a_1^s are used as pure component adjustable parameters and k_{12} , l_{12} , and m_{12} are used as binary adjustable parameters. This equation also estimated the magnitude of the excess volumes of this near-ideal mixture.

Literature Cited

- (1) Riazi, M. R. *Characterization and Properties of Petroleum Fractions*: ASTM: West Conshohocken, PA, 2005.
- (2) Avallée, L.; Neau, E.; Jaubert, J. N. Thermodynamic modeling for petroleum fluid. III. Reservoir fluid saturation pressures. A complete PVT property estimation. Application to swelling test. *Fluid Phase Equilib.* **1997**, *141*, 87–104.
- (3) Audonnet, F.; Pádua, A. A. H. Viscosity and density of mixtures of methane and *n*-decane from 298 to 393 K and up to 75 MPa. *Fluid Phase Equilib.* **2004**, *216*, 235–244.
- (4) Tanaka, Y.; Hosokawa, H.; Kubota, H.; Makita, T. Viscosity and density of binary-mixtures of cyclohexane with *n*-octane, *n*-dodecane, and *n*-hexadecane under high pressures. *Int. J. Thermophys.* **1991**, *12*, 245–264.
- (5) Lemmon, E. W.; McLinden, M. O.; Friend, D. G. Thermophysical properties of fluid systems. In *NIST Chemistry WebBook*, NIST Standard Reference Database No. 69; Linstrom, P. J., Mallard, W. G., Eds.; National Institute of Standards and Technology: Gaithersburg, MD, June 2005 (<http://webbook.nist.gov>).
- (6) Sun, T. F.; Kortbeek, P. J.; Trappeniers, N. J.; Biswas, S. N. Acoustic and thermodynamic properties of benzene and cyclohexane as a function of pressure and temperature. *Phys. Chem. Liq.* **1987**, *16*, 163–178.
- (7) Fandiño, O.; Pensado, A. S.; Lugo, L.; Comuñas, M. J. P.; Fernández, J. Compressed liquid densities of squalane and pentaerythritol tetra-(2-ethylhexanoate). *J. Chem. Eng. Data* **2005**, *50*, 939–946.
- (8) Smith, J. M.; Van Ness, H. C.; Abott, M. M. *Introdução a Termodinâmica da Engenharia Química*; LTC Publisher: Rio de Janeiro, 2000.
- (9) Amorim, J. A.; Chiavone-Filho, O.; Paredes, M. L. L.; Rajagopal, K. High-pressure densities of *n*-hexadecane + cyclohexane mixtures at elevated temperatures: experimental data and modeling. *VII Iberoamerican Conference on Phase Equilibria and Fluid Properties for Process Design*, EQUIFASE, Morélia 2006; v. CD-ROM, 761–772.

Received for review November 7, 2006. Accepted December 29, 2006. The authors acknowledge the financial support from ANP/MCT for the scholarship to J.A.A., MCT/FINEP/CT-PETRO—Temas Estratégicos 01/2006 “Distribuição do Gás Sulfídrico entre Óleos Pesados, Gás Liberado e a Água de Formação nas Condições de Reservatório” Convênio 2528-06 FBR, and PROCAD/CAPES as well as the “bolsa de produtividade” of CNPq to K.R. and O.C.-F.

JE0605036